

INFLUENCE OF DOMAIN WIDTH ON THE THICKNESS AND ENERGY OF SYMMETRIC BLOCH WALLS IN BODY-CENTRED CUBIC FERROMAGNETIC LATTICES

BY J. ULNER

Institute for Low Temperatures and Structural Research, Polish Academy of Sciences, Wrocław*

AND W. J. ZIĘTEK

Institute of Theoretical Physics, University of Wrocław, Wrocław**

and

Institute for Low Temperatures and Structural Research, Polish Academy of Sciences, Wrocław*

(Received March 25, 1968)

The dependence of the thickness and energy of symmetric Bloch walls on the domain width is numerically examined for the case of the *bcc* ferromagnetic lattice, by utilizing the formulae derived for those quantities in an earlier paper (Wachniewski, Ziętek 1967 *Acta Phys. Polon.*, 32, 93 (1967), where the variational principles for the walls were solved under periodic boundary conditions. For each type of wall, the critical domain width is determined below which the departure of the examined quantities from their asymptotic values (as used in the conventional domain theory and in practical applications) becomes significant. As an example, specific data for Fe are provided.

1. Introduction

The variational principles derived in [1] for the various symmetric¹ Bloch walls that may occur in cubic ferromagnetic crystals were solved in [6] for the case of the *bcc* lattice under periodic boundary condition. The solutions thus obtained are expressed in terms of Ja-

* Address: Instytut Niskich Temperatur i Badań Strukturalnych, Polska Akademia Nauk, Wrocław, Plac Katedralny 1, Polska.

** Address: Instytut Fizyki Teoretycznej, Uniwersytet Wrocławski, Wrocław, Cybulskiego 36, Polska.

¹ We use the term "symmetric" for a Bloch wall in which the magnetization vector rotates about the same angle (but in opposite directions) when passing from the wall centre to the centres of the adjacent domains. Since walls of that type are practically the only ones considered in the conventional theory of domain structures, usually they are simply referred to as Bloch walls. However, symmetric walls are merely a special case out of several Bloch wall classes, each containing an infinite number of (generally asymmetric) walls compatible with the magneto-crystalline symmetry of the crystal lattice [2–5]. It was not until very recently that the restriction to symmetric Bloch walls in theoretical considerations has been given a firm justification, by showing the asymmetric walls to be unstable in periodic plate-like domain structures with a screw-like rotation of the magnetization vector on passing through the walls [5]. (See also references in [5] for experimental evidence supporting this conclusion.)

cobi's elliptic functions, the modulus k being a function of material constants and the domain width Δ . The formulae for the thickness δ and the energy σ (per cm²) of the Bloch walls derived in [6] from the periodic solutions involve, generally, the modulus k , the incomplete $F(\varphi, k)$ and complete $\mathbf{K} = \mathbf{K}(k)$ elliptic integrals of the first kind, and the complete elliptic integrals $\mathbf{E} = \mathbf{E}(k)$ and $\mathbf{H}(n, k)$ of the second and third kind, respectively². Since φ and n are in that case functions of k , the thickness δ and the energy σ depend — apart from the material constants — on the domain width Δ , i.e., $\delta = \delta(\Delta)$ and $\sigma = \sigma(\Delta)$.

For all the four types of symmetric Bloch walls considered in [6], the relationship between k and Δ is unique and such that

$$k(\Delta) < k(\Delta') \quad \text{if} \quad \Delta < \Delta', \quad (1)$$

$$\Delta(k) < \Delta(k') \quad \text{if} \quad k < k', \quad (2)$$

$$\lim_{\Delta \rightarrow \infty} k(\Delta) = 1, \quad \lim_{\Delta \rightarrow 0} k(\Delta) = 0, \quad (3)$$

$$\lim_{k \rightarrow 1} \Delta(k) = \infty, \quad \lim_{k \rightarrow 0} \Delta(k) = 0. \quad (4)$$

Hence, the limiting processes $k \rightarrow 0$, $k \rightarrow 1$ and $\Delta \rightarrow 0$, $\infty \Delta \rightarrow \infty$ are respectively equivalent.

For the functions $\delta(\Delta)$ and $\sigma(\Delta)$ derived in [6] — with the corrections given in Appendixes I, II, III of the present paper — one can show that (see also [7, 13])

$$\lim_{\Delta \rightarrow \infty} \frac{\delta}{\Delta} = 0, \quad \lim_{\Delta \rightarrow 0} \frac{\delta}{\Delta} = 1, \quad (5)$$

$$\lim_{\Delta \rightarrow \infty} \delta(\Delta) \equiv \delta_\infty < \infty, \quad \lim_{\Delta \rightarrow 0} \delta(\Delta) = 0, \quad (6)$$

$$\lim_{\Delta \rightarrow \infty} \sigma(\Delta) \equiv \sigma_\infty < \infty, \quad \lim_{\Delta \rightarrow 0} \sigma(\Delta) = \infty, \quad (7)$$

and

$$0 \leq (\delta/\Delta) \leq 1, \quad 0 \leq \delta(\Delta) \leq \delta_\infty, \quad 0 < \sigma_\infty \leq \sigma(\Delta) \leq \infty.$$

The proof that $\delta_\infty < \infty$, and that (δ/Δ) , δ , σ are monotonous functions of Δ , i.e.,

$$\left. \begin{aligned} \delta(\Delta)/\Delta &> \delta(\Delta')/\Delta' \\ \delta(\Delta) &< \delta(\Delta') \\ \sigma(\Delta) &> \sigma(\Delta') \end{aligned} \right\} \text{if} \quad \Delta < \Delta', \quad (8)$$

resides in some cases on mere numerical calculations.

The thickness δ_∞ and the energy σ_∞ defined by Eqs (6), (7) are the so-called asymptotic values (for $\Delta = \infty$) of δ and σ ; as shown in [6, 7, 13], they coincide with the respective quantities obtained from non-periodic solutions [8, 9] of the variational principles, and these asymptotic values are commonly used in practice (see, e.g., [10–12]). Since $\delta \rightarrow 0$ and $\sigma \rightarrow \infty$ as $\Delta \rightarrow 0$, the question arises how large must be the domain width Δ , for a given

² There are however some errors in [1, 6] which are corrected in Appendixes I, II, III of the present paper. In particular, a systematic error has been made in calculating the wall energies $\sigma(\Delta)$ in [6]; the correct formulae are given in Appendix III.

material and a particular Bloch wall, in order that the asymptotic values δ_∞ and σ_∞ be fairly accurate approximations of the exact ones $\delta(\Delta)$ and $\sigma(\Delta)$. A rough estimation of the difference $\sigma(\Delta) - \sigma_\infty$ was carried through in [7] where an inequality of the form

$$0 < \sigma(\Delta) - \sigma_\infty < \frac{\text{const}}{\Delta} \quad (9)$$

was derived. More subtle estimates confined, however, to the function $\delta(\Delta)$ were presented in [13], leading to the approximate formula

$$\Delta_c = 10\delta_\infty \quad (10)$$

for the critical domain width Δ_c below which $\delta/\Delta > 0.1$. In the present paper, the results of a systematic numerical analysis are given showing the dependence of δ/δ_∞ , σ/σ_∞ and δ/Δ on Δ in the region where the departure of δ and σ from their asymptotic values becomes significant.

Following the notation introduced in [1] and refined in [13], the symbol $(\Psi[xyz]\Phi)$ shall be used in denoting the type of symmetric Bloch wall, where $[xyz]$ is the crystallographic direction normal to the wall (rotation axis of the magnetization vector), Ψ the angle between the directions of the magnetization vector at the centres of adjacent domains, and Φ the angle by which the magnetization vector rotates on passing through the wall in the direction $[xyz]$ over a distance equal to the domain width Δ . There are four types of symmetric Bloch walls in the *bcc* lattice, namely, the $(90^\circ[100]90^\circ)$, $(90^\circ[101]180^\circ)$, $(180^\circ[110]180^\circ)$, and $(90^\circ[111]120^\circ)$ Bloch wall. All these Bloch walls were considered in [6] (and, in the asymptotic approximation, in [8, 9]) and shall be examined numerically in the present paper. In carrying out the numerical calculations, we used the tables [14, 15]. No models of the Bloch walls are given here, as they can be found in [6].

2. Numerical calculations

The microscopic material constants A , K , a , S used in [1, 6] and denoting respectively the (negative) exchange integral, the microscopic anisotropy constant, the lattice constant, and the maximum spin eigenvalue, can for the *bcc* lattice be replaced by the conventional macroscopic (positive) exchange constant A^{bcc} and the first (phenomenological) anisotropy constant K_1^{bcc} as follows [9, 13]:

$$A^{bcc} = -2a^{-1}AS^2, \quad K_1^{bcc} = 2a^{-3}KS^2 \left(S - \frac{1}{2} \right)^2. \quad (11)$$

Upon introducing the quantities

$$\delta_0 = \sqrt{A^{bcc}|K_1^{bcc}|}, \quad \sigma_0 = \sqrt{A^{bcc}K_1^{bcc}} \quad (12)$$

depending on the material and having respectively the dimensions of length and energy per surface area the formulae derived in [6] for the energy σ and thickness δ of the Bloch walls, as well as the relations between the domain width Δ and the modulus k can for each

Bloch wall be written in the form

$$\Delta = \delta_0 D(k), \quad \delta = \delta_0 d(k), \quad \sigma = \sigma_0 f(k), \quad (13)$$

where D , d and f are dimensionless functions of the modulus k only which characterize the type of symmetric Bloch wall regardless of the material. Accordingly, the asymptotic values δ_∞ and σ_∞ defined by Eqs (6) and (7) follow from Eq. (13) for $k \rightarrow 1$, *i.e.*,

$$\begin{aligned} \delta_\infty &= \delta_0 \lim_{k \rightarrow 1} d(k) \equiv \delta_0 d(1), \\ \sigma_\infty &= \sigma_0 \lim_{k \rightarrow 1} f(k) \equiv \sigma_0 f(1), \end{aligned} \quad (14)$$

and the functions to be numerically examined in the present paper are the dimensionless ratios

$$\frac{\delta}{\delta_\infty} = \frac{d(k)}{d(1)}, \quad \frac{\sigma}{\sigma_\infty} = \frac{f(k)}{f(1)}, \quad \frac{\delta}{\Delta} = \frac{d(k)}{D(k)} \equiv R(k), \quad (15)$$

of which the first two describe the departure of δ and σ from their asymptotic values δ_∞ and σ_∞ with decreasing domain width Δ , while the last one illustrates the gradual transition of the well-defined domain structure for large Δ (with domains much wider than the narrow, sharply pronounced Bloch walls separating them) to a spiral-like magnetic structure for small Δ which renders the very notion of domains and walls meaningless, as in the limit case $k \rightarrow 0$ the rotation angle of the magnetization vector becomes a linear function of the distance measured along the crystallographic direction normal to the walls, thus "walls" being indistinguishable from "domains".

The qualitative behaviour of the ratios (15) has already been studied in [6, 7, 13]. For the quantitative examination in the present paper, the relation between Δ and k in Eq. (13) is in each case the starting point for the calculations, and, since k is an involved function of Δ , this relation has been used in determining Δ for specific values of k . The numerical calculations were carried through by determining the functions $D(k)$, $d(k)$ and $f(k)$ for such values of k from the whole interval $0 \leq k \leq 1$ for which the numerical values of the various elliptic integrals entering in $D(k)$, $d(k)$ and $f(k)$ are available [14]. In this way, the ratios (15) could be determined with an accuracy usually better than 1%.

In the diagrams presented here, the ratios (15) are plotted as functions of the domain width Δ . In order that our results be applicable to any material, Δ is measured in δ_0 as unit length which, along with σ_0 , is to be specified for each material. For instance, according to [11], p. 293, one has³ for Fe (at room temperature)

$$\begin{aligned} A^{bcc} &= 8.3 \times 10^{-7} \text{ erg/cm}, & K_1^{bcc} &= 5.3 \times 10^5 \text{ erg/cm}^3, \\ \delta_0 &= 125 \text{ \AA}, & \sigma_0 &= 0.66 \text{ erg/cm}^2. \end{aligned} \quad (16)$$

³ It is to be noted that the accuracy in determining experimentally the material constants — particularly A^{bcc} — is still very poor, which results in remarkable differences between the values quoted by different authors. For example, according to [12], p. 53, we have for Fe at room temperature $A^{bcc} = 25 \times 10^{-7} \text{ erg/cm}$, $K_1^{bcc} = 4.6 \times 10^5 \text{ erg/cm}^3$, which leads to $\delta_0 = 260 \text{ \AA}$, $\sigma_0 = 1.07 \text{ erg/cm}^2$, *i. e.*, about twice the values from Eq. (16).

Each diagram is supplemented by a table containing a selected set of numerical data for the ratios (15), so that each curve can be reconstructed for practical purposes. Moreover, specific results for Fe are provided to illustrate the dependence of δ and σ on Δ for a typical three-axial ferromagnet with *bcc* lattice.

a) The ($90^\circ[100] 90^\circ$) Bloch wall

From Eq. (11) in [6] we have the relation between the domain width Δ and the modulus k

$$k^2 \mathbf{K}^2 = 2u_4 \Delta^2 / u_0, \quad (17)$$

with the coefficients

$$u_0 = -a^2 A S^2, \quad u_4 = \frac{1}{8} K S^2 \left(S - \frac{1}{2} \right)^2 \quad (18)$$

from Table I in [6]. Upon passing to the macroscopic material constants (11) we obtain

$$\Delta = 2\delta_0 k \mathbf{K} \equiv \delta_0 D(k) \quad (19)$$

with δ_0 defined by Eq. (12). Similarly, we have from Eq. (13) in [16]

$$\delta = \pi \delta_0 k \equiv \delta_0 d(k), \quad (20)$$

and from Eq. (III.12) in Appendix III

$$\sigma = \sigma_0 \{ 2\mathbf{E} - (1-k^2)\mathbf{K} \} / 2k \equiv \sigma_0 f(k) \quad (21)$$

with σ_0 as defined by Eq. (12).

The limit values for $k \rightarrow 0$ and $k \rightarrow 1$ of the functions $d(k)$, $D(k)$, $f(k)$ and $R(k) = d(k)/D(k)$ from Eqs (19)–(21) are easily calculated:

$$\begin{aligned} d(0) = D(0) = R(1) = 0, \quad R(0) = f(1) = 1, \\ d(1) = \pi, \quad D(1) = f(0) = \infty. \end{aligned} \quad (22)$$

This proves Eqs (3)–(7) and, due to Eqs (14), (20) and (21), leads to

$$\delta_\infty = \pi \delta_0, \quad \sigma_\infty = \sigma_0. \quad (23)$$

For Fe we obtain from Eqs (16) and (23)

$$\delta_\infty = 393 \text{ \AA}, \quad \sigma_\infty = 0.66 \text{ erg/cm}^2. \quad (24)$$

According to Eqs (19)–(22) the ratios (15) take the form

$$\frac{\delta}{\delta_\infty} = k, \quad \frac{\sigma}{\sigma_\infty} = f(k), \quad \frac{\delta}{\Delta} = \frac{\pi}{2\mathbf{K}} \quad (25)$$

with $f(k)$ from Eq. (21). These ratios are involved functions of Δ , as k is an involved function of Δ defined by Eq. (19).

The dependence of the ratios (25) on Δ (in units of δ_0) is shown in Fig. 1. A representative set of numerical data is given in Table I, along with specific results for Fe. The first two columns show the dependence of Δ on k (or vice versa), according to Eq. (19).

b) The ($180^\circ[110]180^\circ$) Bloch wall

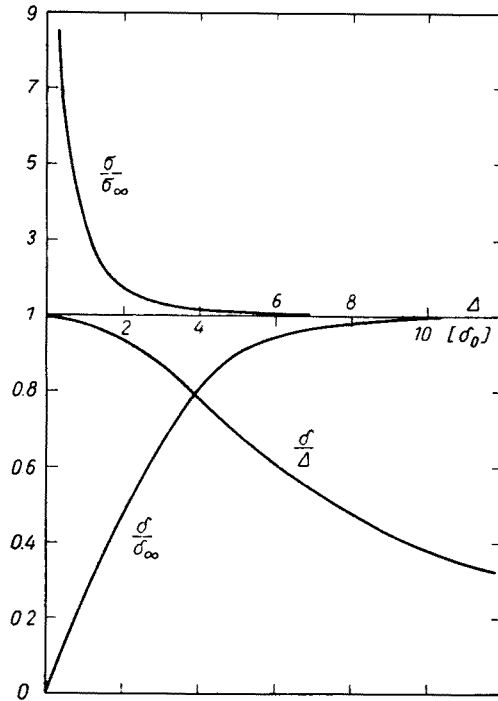


Fig. 1. Curves of the ratios (15) as defined by Eq. (25) for the $(90^\circ|100|90^\circ)$ and $(90^\circ|111|120^\circ)$ symmetric Bloch walls (cp. Table I)

TABLE I

Representative set of numerical data for Δ/δ_0 and the ratios (15) as defined by Eqs (19), (25) for the $(90^\circ|100|90^\circ)$ and $(90^\circ|111|120^\circ)$ symmetric Bloch walls (cp. Fig. 1), with results specified for Fe in the last four columns

k^2	$\frac{\Delta}{\delta_0}$	$\frac{\delta}{\delta_\infty}$	$\frac{\delta}{\Delta}$	$\frac{\sigma}{\sigma_\infty}$	Fe			
					$\Delta[\text{\AA}]$	$\delta[\text{\AA}]$	$\sigma [\text{erg/cm}^2]$	
							$(90^\circ 90^\circ)$	$(90^\circ 120^\circ)$
0	0	0	1	∞	0	0	∞	∞
0.01	0.31	0.100	0.997	7.87	40	40	5.2	6.1
0.1	1.02	0.316	0.974	2.55	128	124	1.7	2.0
0.3	1.87	0.548	0.916	1.54	234	215	1.0	1.2
0.5	2.62	0.707	0.847	1.25	328	278	0.83	0.98
0.7	3.48	0.837	0.756	1.11	435	329	0.73	0.87
0.9	4.90	0.949	0.609	1.03	613	373	0.68	0.80
0.95	5.68	0.975	0.540	1.01	710	383	0.67	0.79
0.99	7.36	0.995	0.425	1.00	920	391	0.66	0.78
1	∞	1	0	1	∞	393	0.66	0.78

According to Table I in [6], the coefficients u_0 , u_2 and u_4 for this wall read

$$u_0 = -a^2 AS^2, \quad u_2 = \frac{4}{3} u_4 = \frac{1}{8} KS^2 \left(S - \frac{1}{2} \right)^2. \quad (26)$$

By utilizing Eqs (11) and (12), the relation (28) in [6] between Δ and k can be written in the form

$$\Delta = 8\delta_0 \mathbf{K} / \sqrt{3+\omega} \equiv \delta_0 D(k) \quad (27)$$

where $\omega = \omega(k)$ is defined by the equality (see Eq. (37) in [6])

$$k^2 = (3\omega + 1) / \omega(3 + \omega). \quad (28)$$

Similarly, by the aid of Eqs (11), (12) and (26) we obtain from the corrected formulae (II.2) in Appendix II and (III.16) in Appendix III the Bloch wall thickness

$$\delta = 4\delta_0 \left\{ \mathbf{K} - F \left(\theta - \frac{\pi}{2}, k \right) + 2\vartheta \sqrt{3\omega/(1+3\omega)} \right\} / \sqrt{3+\omega} \equiv \delta_0 d(k) \quad (29)$$

and the Bloch wall energy

$$\sigma = \sigma_0 \sqrt{3+\omega} \left\{ \mathbf{E} + \frac{\omega-1}{2\omega(3+\omega)} [2(\omega+1)\mathbf{E}(-\omega^{-2}, k) - (3\omega+1)\mathbf{K}] \right\} \equiv \sigma_0 f(k), \quad (30)$$

where

$$\tan \vartheta = \sqrt{2}, \quad 2\vartheta \approx 109^\circ, \quad (31)$$

$$\tan \theta = -2\sqrt{2(\omega^2-1)/(3+\omega)}, \quad 2\vartheta \leq \theta \leq \pi$$

from Eqs (31), (33) and (38) in [6].

It was shown in [6] that

$$\begin{aligned} \lim_{k \rightarrow 0} \omega(k) &= \infty, & \lim_{k \rightarrow 1} \omega(k) &= 1, \\ \lim_{k \rightarrow 0} \theta(k) &= 2\vartheta, & \lim_{k \rightarrow 1} \theta(k) &= \pi. \end{aligned} \quad (32)$$

Hence, for $k \rightarrow 0$ and $k \rightarrow 1$ one easily obtains the limit values of $d(k)$, $D(k)$, $f(k)$ and $R(k) = d(k)/D(k)$ as defined by Eqs (27)–(30):

$$d(0) = D(0) = R(1) = 0, \quad R(0) = 1, \quad D(1) = f(0) = \infty. \quad (33)$$

As for $d(1)$ and $f(1)$, we take the asymptotic values δ_∞ and σ_∞ derived for this wall in [9a] (see Eqs (26)–(28) therein) and make use of the fact that $\sigma \rightarrow \sigma_\infty$ as $\Delta \rightarrow \infty$ according to [7], and that $\delta \rightarrow \delta_\infty$ as $\Delta \rightarrow \infty$ according to our numerical calculations (cp. Fig. 2 and Table II). Hence we conclude

$$\begin{aligned} d(1) &= 2 \ln(\sqrt{3}+2) + 2\sqrt{3} \sin^{-1} \sqrt{2/3} \approx 5.59, \\ f(1) &= 2 + (\sqrt{3}/3) \tanh^{-1}(\sqrt{3}/2) \approx 2.76 \end{aligned} \quad (34)$$

which, together with Eq. (33), proves Eqs (3)–(7) and, due to Eqs (14), (29) and (30), leads to

$$\delta_{\infty} = 5.59 \delta_0, \quad \sigma_{\infty} = 2.76 \sigma_0. \quad (35)$$

For Fe we obtain from Eqs (16) and (35)

$$\delta_{\infty} = 700 \text{ \AA}, \quad \sigma_{\infty} = 1.82 \text{ erg/cm}^2. \quad (36)$$

According to Eq. (34), the ratios (15) take the form

$$\frac{\delta}{\delta_{\infty}} = 0.179 d(k), \quad \frac{\sigma}{\sigma_{\infty}} = 0.362 f(k), \quad \frac{\delta}{\Delta} = \frac{d(k)}{D(k)} \quad (37)$$

with $D(k)$, $d(k)$ and $f(k)$ from Eqs (27), (29) and (30). Their involved dependence on Δ is given by Eqs (27) and (28).

Fig. 2 shows the ratios (37) as functions of Δ (in units of δ_0). Tables II and III contain representatives sets of numerical data, along with specific results for Fe. Since in the present case the function $d(k)$ contains an incomplete elliptic integral of the first kind, and $f(k)$ contains a complete elliptic integral of the third kind, the ratios δ/δ_{∞} , δ/Δ and the ratio σ/σ_{∞} had to be calculated separately, in order that each ratio be computed with the same accuracy. Thus, in the first case the angle θ has been chosen as independent variable and

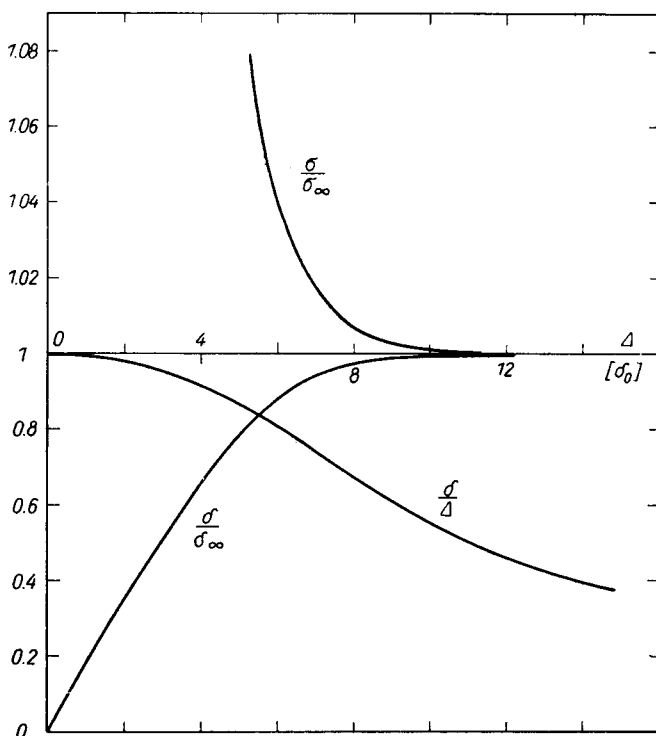


Fig. 2. Curves of the ratios (15) as defined by Eq. (37) for the $(180^\circ[110]180^\circ)$ symmetric Bloch wall (cp. Tables II and III)

TABLE II

Representative set of numerical data for Δ/δ_0 , δ/δ_∞ and δ/Δ as defined by Eqs (27), (37) for the $(180^\circ[110]180^\circ)$ symmetric Bloch wall (cp. Fig. 2), with results specified for Fe in the last two columns

$\theta-90^\circ$	ω	k^2	$\frac{\Delta}{\delta_0}$	$\frac{\delta}{\delta_\infty}$	$\frac{\delta}{\Delta}$	Fe	
						$\Delta[\text{\AA}]$	$\delta[\text{\AA}]$
$2\theta-90^\circ$	∞	0	0	0	1	0	0
20°	100.46	0.03	1.24	0.220	0.990	155	154
25°	9.62	0.25	3.79	0.626	0.924	474	438
30°	5.00	0.40	5.03	0.779	0.868	629	545
35°	3.37	0.52	5.93	0.876	0.827	741	613
48°	1.84	0.73	7.73	0.957	0.697	966	670
58°	1.39	0.85	9.07	0.990	0.608	1130	693
82°	1.02	0.99	14.72	0.992	0.377	1840	694
90°	1	1	∞	1	0	∞	700

TABLE III

Representative set of numerical data for Δ/δ_0 and σ/σ_∞ as defined by Eqs (27), (37) for the $(180^\circ[110]180^\circ)$ symmetric Bloch wall (cp. Fig. 2), with results specified for Fe in the last two columns

ω^{-2}	k^2	$\frac{\Delta}{\delta_0}$	$\frac{\sigma}{\sigma_\infty}$	Fe	
				$\Delta[\text{\AA}]$	$\sigma[\text{erg/cm}^2]$
0	0	0	∞	0	∞
0.05	0.431	5.27	1.078	659	1.96
0.10	0.538	6.08	1.039	760	1.89
0.30	0.735	7.76	1.009	970	1.84
0.50	0.840	8.98	1.003	1120	1.83
0.70	0.915	10.32	1.001	1290	1.82
0.90	0.974	12.81	1.000	1600	1.82
1	1	∞	1	∞	1.82

the corresponding values of ω , k and Δ have been determined from Eqs (31), (28) and (27). In the second case the values for ω have been fixed in advance and the corresponding values of k and Δ have been determined from Eqs (28) and (27). This explains the different sets of numerical data for k^2 , Δ/δ_0 and Δ in Tables II and III which is, of course, immaterial as regards the final results (curves in Fig. 2). In particular, the data from the third and fourth column in Table II and from the second and third column in Table III lead to the same curve for $\Delta(k)$ as defined by Eq. (27) (curve not given here).

c) The $(90^\circ[101]180^\circ)$ Bloch wall

From Table I in [6], the coefficients u_0 , u_2 and u_4 for this wall read

$$u_0 = -\frac{1}{2}a^2AS^2, \quad u_2 = \frac{20}{3}u_4 = \frac{5}{32}KS^2\left(S - \frac{1}{2}\right)^2 \quad (38)$$

and, upon introducing δ_0 and σ_0 as defined by Eqs (11) and (12), the relation (52) in [6] between Δ and k can be written in the form

$$= 8\sqrt{2}\delta_0\mathbf{K}/\sqrt{3+5\omega} \equiv \delta_0 D(k), \quad (39)$$

where $\omega = \omega(k)$ is defined by the equality

$$k^2 = (5+3\omega)/\omega(5\omega+3) \quad (40)$$

which follows from Eq. (50) in [6].

Quite similarly, Eq. (53) in [6] for δ and Eq. (III.20) in Appendix III for σ can be expressed in the form

$$\delta = 4\pi\delta_0\sqrt{2\omega/5}/(\omega+1) \equiv \delta_0 d(k), \quad (41)$$

$$\sigma = \frac{\sigma_0}{4}\sqrt{2(5\omega+3)}\left\{\mathbf{E} + \frac{5(\omega-1)}{2\omega(5\omega+3)}[2(\omega+1)\mathbf{II}(-\omega^{-2}, k) - (3\omega+1)\mathbf{K}]\right\} \equiv \sigma_0 f(k) \quad (42)$$

when making use of Eqs (11), (12) and (38).

From Eq. (51) in [6] one easily proves that

$$\lim_{k \rightarrow 0} \omega(k) = \infty, \quad \lim_{k \rightarrow 1} \omega(k) = 1, \quad (43)$$

which permits to determine the limit values for $k \rightarrow 0$ and $k \rightarrow 1$ of the functions $D(k)$, $d(k)$, $f(k)$ and $R(k) = d(k)/D(k)$ defined by Eqs. (39)–(42):

$$\begin{aligned} d(0) = D(0) = R(1) = 0, \quad R(0) = 1, \\ f(0) = D(1) = \infty, \quad d(1) = 2\pi\sqrt{2/5} \approx 3.97. \end{aligned} \quad (44)$$

To determine $f(1)$, we note that $\sigma \rightarrow \sigma_\infty$ for $\Delta \rightarrow \infty$, as shown in [7], and take σ_∞ from Eq. (36) in [9a]. In this way we obtain

$$f(1) = 1 + (5/2\sqrt{6}) \tanh^{-1}\sqrt{3/8} \approx 1.73 \quad (45)$$

which, together with Eq. (44), proves Eqs (3)–(7) and, due to Eqs (14), (41) and (42) leads to

$$\delta_\infty = 3.97 \delta_0, \quad \sigma_\infty = 1.73 \sigma_0. \quad (46)$$

For Fe we have from Eqs (16) and (46)

$$\delta_\infty = 495 \text{ \AA}, \quad \sigma_\infty = 1.14 \text{ erg/cm}^2. \quad (47)$$

According to Eqs (44) and (45) we have for the ratios (15)

$$\frac{\delta}{\delta_\infty} = 0.252 d(k), \quad \frac{\sigma}{\sigma_\infty} = 0.578 f(k), \quad \frac{\delta}{\Delta} = \frac{d(k)}{D(k)} \quad (48)$$

with $D(k)$, $d(k)$ and $f(k)$ from Eqs (39)–(42). These ratios depend on Δ as shown in Fig. 3. A representative set of numerical data is given in Table IV, along with specific results for Fe.

d) The $(90^\circ[111]120^\circ)$ Bloch wall

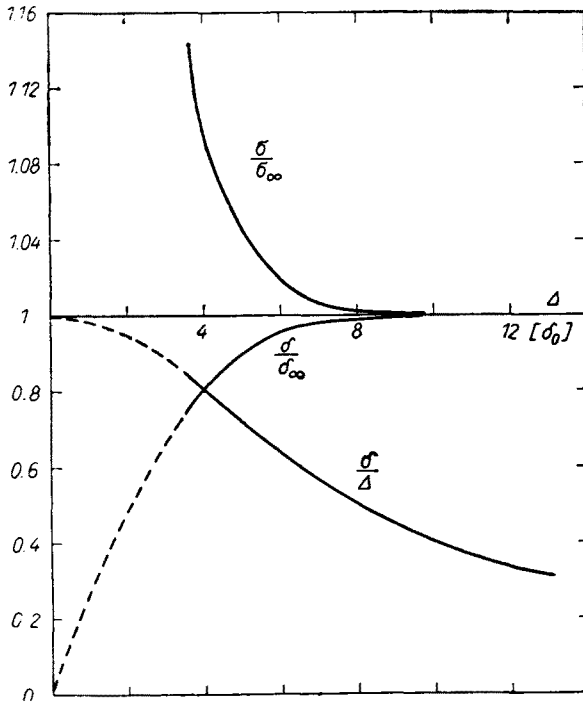


Fig. 3. Curves of the ratios (15) as defined by Eq. (48) for the $(90^\circ[101]180^\circ)$ symmetric Bloch wall (cp. Table IV)

TABLE IV

Representative set of numerical data for Δ/δ_0 and the ratios (15) as defined by Eqs (39), (48) for the $(90^\circ[101]180^\circ)$ symmetric Bloch wall (cp. Fig. 3), with results specified for Fe in the last three columns

ω^{-2}	k^2	$\frac{\Delta}{\delta_0}$	$\frac{\delta}{\delta_\infty}$	$\frac{\delta}{\Delta}$	$\frac{\sigma}{\sigma_\infty}$	Fe		
						$\Delta[\text{\AA}]$	$\delta[\text{\AA}]$	$\sigma \left[\frac{\text{erg}}{\text{cm}^2} \right]$
0	0	0	0	1	∞	0	0	∞
0.05	0.162	3.68	0.773	0.833	1.14	460	383	1.30
0.1	0.244	4.38	0.855	0.774	1.07	548	423	1.22
0.3	0.473	5.94	0.956	0.639	1.02	743	473	1.16
0.5	0.649	7.15	0.985	0.548	1.01	894	488	1.15
0.7	0.800	8.50	0.996	0.465	1.00	1060	493	1.14
0.9	0.936	10.91	0.999	0.362	1.00	1360	495	1.14
1	1	∞	1	0	1	∞	495	1.14

The relation between Δ and k for this wall given by Eq. (64) in [6] is

$$k^2 \mathbf{K}^2 = 9u_3 \Delta^2 / 8u_0, \quad (49)$$

with the coefficient u_3 from Table I in [6] and u_0 from Eq. (I.4) in Appendix I, *i.e.*,

$$u_0 = -\frac{2}{3} a^2 A S^2, \quad u_3 = \frac{4}{27} K S^2 \left(S - \frac{1}{2} \right)^2. \quad (50)$$

In terms of δ_0 as defined by Eqs (11) and (12) relation (49) reads

$$\Delta = 2\delta_0 k \mathbf{K} \equiv \delta_0 D(k). \quad (51)$$

Similarly, Eq. (65) in [6] for δ and Eq. (III.22) in Appendix III for σ can be written in the form

$$\delta = \pi \delta_0 k \equiv \delta_0 d(k), \quad (52)$$

$$\sigma = \frac{32}{27} \sigma_0 \{ 2\mathbf{E} - (1-k^2)\mathbf{K} \} / 2k \equiv \sigma_0 f(k). \quad (53)$$

When comparing Eqs (51)–(53) with Eqs (19)–(21) one sees that the functions $D(k)$, $d(k)$ and $R(k) = d(k)/D(k)$ are identical, and that $f(k)$ differs merely by the coefficient $32/27$. Therefore, the limit values are the same as in Eq. (22) except that now

$$f(1) = \frac{32}{27} \approx 1.19 \quad (54)$$

which slightly changes σ_∞ :

$$\sigma_\infty = 1.19\sigma_0, \quad \text{for Fe: } \sigma_\infty = 0.78 \text{ erg/cm}^2. \quad (55)$$

This, however, has no influence on the ratio σ/σ_∞ . Hence, the ratios (15) are for the $(90^\circ[111]120^\circ)$ Bloch wall the same as for the $(90^\circ[100]90^\circ)$ Bloch wall, Eq. (25), and therefore lead to the same curves as in Fig. 1, the only difference being in that — for the same domain width Δ — the energy σ' of the $(90^\circ[111]120^\circ)$ wall is 1.19 times larger than that of the $(90^\circ[100]90^\circ)$ wall, as seen from the last two columns in Table I for Fe.

3. Concluding remarks

It is seen from Figs 1–3 and Tables I–IV that a significant departure of δ and σ from their asymptotic values δ_∞ and σ_∞ occurs for all the Bloch walls for comparatively small domain widths Δ , despite the fact that in this region the Bloch wall thickness δ and the domain width Δ are already of the same order of magnitude. This is best illustrated by the Tables V–VII. From Table V we see that a 10% contraction of the Bloch wall thicknesses takes place in the region from $4\delta_0$ to $6.5\delta_0$ for the domain width, which for Fe corresponds to the interval $500 \text{ \AA} - 800 \text{ \AA}$. The increase of the Bloch wall energies in this region is even smaller, from 2% to 6% of the asymptotic values, while at the same time $0.7 \leq (\delta/\Delta) \leq 0.8$, *i.e.*, the Bloch wall thicknesses amount already from 70% to 80% of the corresponding

TABLE V

Approximate values of Δ/δ_0 , δ/Δ and σ/σ_∞ for $(\delta/\delta_\infty) = 0.9$

Type of wall	$\frac{\Delta}{\delta_0}$	$\frac{\delta}{\Delta}$	$\frac{\sigma}{\sigma_\infty}$	Fe		
				$\Delta[\text{\AA}]$	$\delta[\text{\AA}]$	$\sigma [\text{erg/cm}^2]$
(90°[100]90°)	4.1	0.7	1.06	500	350	0.7
(180°[110]180°)	6.5	0.8	1.02	800	640	1.9
(90°[101]180°)	5.1	0.7	1.05	600	420	1.2
(90°[111]120°)	4.1	0.7	1.06	500	350	0.8

TABLE VI

Approximate values of Δ/δ_0 , δ/Δ and δ/δ_∞ for $(\sigma/\sigma_\infty) = 1.1$

Type of wall	$\frac{\Delta}{\delta_0}$	$\frac{\delta}{\Delta}$	$\frac{\delta}{\delta_\infty}$	Fe		
				$\Delta[\text{\AA}]$	$\delta[\text{\AA}]$	$\sigma[\text{erg/cm}^2]$
(90°[100]90°)	3.5	0.75	0.84	440	330	0.73
(180°[110]180°)	5.0	0.88	0.78	630	565	2.00
(90°[101]180°)	3.3	0.81	0.81	490	395	1.25
(90°[111]120°)	3.5	0.75	0.84	440	330	0.86

TABLE VII

Approximate values of Δ/δ_0 , δ/δ_∞ and σ/σ_∞ for $(\delta/\Delta) = 0.5$

Type of wall	$\frac{\Delta}{\delta_0}$	$\frac{\delta}{\delta_\infty}$	$\frac{\sigma}{\sigma_\infty}$	Fe		
				$\Delta[\text{\AA}]$	$\delta[\text{\AA}]$	$\sigma[\text{erg/cm}^2]$
(90°[100]90°)	6.3	0.98	1.01	770	385	0.67
(180°[110]180°)	11.2	0.99	1.00	1390	695	1.82
(90°[101]180°)	7.9	0.99	1.00	980	490	1.14
(90°[111]120°)	6.3	0.98	1.01	770	385	0.79

domain widths. As seen from Table VI, the situation is much the same for a 10% increase of the Bloch wall energies. On the other hand, Table VII shows that δ and σ differ from their asymptotic values by at most 2% for $\delta/\Delta = 0.5$, the domain width in this instance ranging from $6.3\delta_0$ to $11.2\delta_0$, that is for Fe from 770 Å to 1390 Å. This means that for domain widths larger than $6.3\delta_0$, $11.2\delta_0$ and $7.9\delta_0$ for the respective Bloch walls the asymptotic values δ_∞ and σ_∞ are very good approximations of the exact ones δ and σ , in spite of the fact that the thickness of the wall may actually be as large as half the domain width.

Finally, we would like to point out that our curves and numerical data can be used in determining experimentally the Bloch wall thickness and energy for domain widths smaller than the critical values given in the first column in Table VII, by simply measuring the domain width which even in this region remains the only quantity easily accessible to measurements.

APPENDIX I

When deriving the variational principle for the $(90^\circ[111]120^\circ)$ symmetric Bloch wall in [1], a coefficient $1/9$ has been omitted while transforming the bilinear part of the Hamiltonian into the form (48). The coefficient $3A^{\alpha\beta}$ in this formula should be replaced by $A^{\alpha\beta}/3$, i.e., Eq. (48) in [1] should read

$$\tilde{P}_{33}^{\alpha\beta} = \frac{1}{3} A^{\alpha\beta} \{1 + 2 \cos(\varphi^\alpha - \varphi^\beta)\}. \quad (\text{I.1})$$

Consequently, the exchange integral A in Eqs (50), (51), (53) in [1] should be replaced by $A/3$ and these formulae should respectively read

$$h = C - \frac{1}{3} AS^2 \sum_{\alpha\beta} \dots \text{etc.}, \quad (\text{I.2})$$

$$C = NS^2 \{\gamma A + \dots \text{etc.}, \quad (\text{I.3})$$

$$u_0 = -\frac{2}{3} a^2 AS^2 > 0. \quad (\text{I.4})$$

Accordingly, the coefficient $-u_0/a^2 AS^2$ for this wall in Table I in [6] (first row, last column) should read $2/3$ instead of $[6]$.

APPENDIX II

A coefficient $1/2$ has been omitted in Eq. (34) in [6] when calculating the thickness δ of the $(180^\circ[110]180^\circ)$ symmetric Bloch wall. Correctly, this equation should read

$$\begin{aligned} & \left\{ \xi \left(\varphi = \frac{\pi}{2} \right) - \xi(\varphi = \vartheta) \right\} = \dots \\ & = \frac{1}{2} \sqrt{2u_0/u_2(3+\omega)} \int_{\vartheta - \pi/2}^{\pi/2} [1 - k^2 \sin^2 \Phi]^{-1/2} d\Phi \quad (\text{II.1}) \\ & = \frac{1}{2} \sqrt{2u_0/u_2(3+\omega)} \left\{ \mathbf{K} - F \left(\theta - \frac{\pi}{2}, k \right) \right\} \end{aligned}$$

which slightly changes the resulting formula for δ , Eq. (36) in [6], to

$$\delta = \sqrt{2u_0/u_2(3+\omega)} \left\{ \mathbf{K} - F \left(\theta - \frac{\pi}{2}, k \right) + 2\vartheta \sqrt{3\omega/(1+3\omega)} \right\}. \quad (\text{II.2})$$

APPENDIX III

A systematic error has been made in [6] when calculating the energies σ for all the four Bloch walls. According to the definition given by Eq. (14) in [6] one has

$$\sigma = \Delta(h_\varphi - h_0)/V \quad (\text{III.1})$$

where Δ is the domain width and V the volume of the crystal. The quantities h_φ and h_0 are particular values of the functional $h[\varphi]$ which for all the Bloch walls considered in [6] can be written in the form (see Eq. (1) in [6])

$$\begin{aligned} h[\varphi] &= \text{const} + 2a^{-3} \int_V \{u_0 \dot{\varphi}^2 - u_2 \cos 2\varphi - u_3 \cos 3\varphi - u_4 \cos 4\varphi\} dv \\ &\equiv \text{const} + 2a^{-3} \int_V f(\varphi, \dot{\varphi}) dv, \end{aligned} \quad (\text{III.2})$$

where $\varphi = \varphi(\xi)$, $\dot{\varphi} = d\varphi/d\xi$. Since the integrand f does not depend explicitly on the variable ξ , the Euler-Lagrange equation for the functional $h[\varphi]$ can be written in the form of a first-order differential equation:

$$\dot{\varphi} \frac{\partial f}{\partial \dot{\varphi}} - f = C, \quad (\text{III.3})$$

that is,

$$u_0 \dot{\varphi}^2 + u_2 \cos 2\varphi + u_3 \cos 3\varphi + u_4 \cos 4\varphi = C, \quad (\text{III.4})$$

where C is the first integration constant (to be determined from the boundary conditions).

By definition, h_φ in Eq. (III.1) is the value of the functional (III.2) upon inserting the solution of the Euler-Lagrange equation (III.4), *i.e.*,

$$\begin{aligned} h_\varphi &\equiv \text{const} + NC + 4a^{-3} \int_V \{u_2 \cos 2\varphi + u_3 \cos 3\varphi + u_4 \cos 4\varphi\} dv \\ &\equiv \text{const} + NC - \tilde{h}_\varphi \end{aligned} \quad (\text{III.5})$$

where N is the number of lattice atoms ($N = 2V/a^3$ for the *bcc* lattice). Analogously, by definition h_0 is the value of the functional (III.2) for $\varphi = \dot{\varphi} = 0$, *i.e.*,

$$\begin{aligned} h_0 &= \text{const} + 2a^{-3} \int_V f(0,0) dv \\ &= \text{const} + Nf(0,0) \end{aligned} \quad (\text{III.6})$$

where

$$f(0,0) = -(u_2 + u_3 + u_4) \quad (\text{III.7})$$

from Eq. (III.2).

It must be noted that, generally, one should write h_α instead of h_0 in the definition (III.1) and define h_α as the value of the functional $h[\varphi]$ for $\dot{\varphi} = 0$, $\varphi = \alpha$, the angle α corresponding to the direction of magnetization at any domain centre or, equivalently, to any direction of easiest magnetization. This is because h_0 , or h_α , is actually meant to represent the so-called "isotropic background energy" corresponding to the case when no Bloch walls are present, *i.e.*, when a single domain extends all over the crystal and hence the crystal is spontaneously magnetized to saturation in any direction of easiest magnetization. Since for all the walls considered in [6], as well as in [16], the rotations of the magnetization vector have been so specified that $\varphi = 0$ always corresponds to a direction of easiest magnetization, our definition (III.1) is specified accordingly.

By inserting Eqs (III.5) and (III.6) into Eq. (III.1) we obtain

$$\sigma = \frac{\Delta}{V} \{NC - Nf(0,0) - \tilde{h}_\varphi\}. \quad (\text{III.8})$$

Due to an oversight, the Bloch wall energies in [6, 16] have been calculated from the erroneous formula

$$\sigma' = -\frac{\Delta}{V} \{2Nf(0,0) + \tilde{h}_\varphi\} \quad (\text{III.9})$$

which is correct for the limit case $\Delta \rightarrow \infty$ only and, fortunately, differs from (III.8) merely by a simple additive term, *i.e.*,

$$\sigma = \sigma' + \frac{N\Delta}{V} \{C + f(0,0)\} \equiv \sigma' + c. \quad (\text{III.10})$$

This term is easily calculated, as the constants from Eqs (10), (25), (49) and (63) in [6] for the respective Bloch walls are simply equal to C/u_0 , the domain width Δ can be expressed through the modulus k and the complete elliptic integral of the first kind \mathbf{K} from Eqs (11), (28), (52), and (64) in [6], respectively, and $f(0,0)$ as defined by (III.7) can readily be specified for each Bloch wall from Table I in [6]. Taking into account that $N/V = 2a^{-3}$ for the *bcc* lattice we thus have:

For the $(90^\circ[100]90^\circ)$ Bloch wall:

$$\begin{aligned} C &= u_4(2-k^2)/k^2, & \Delta &= k\mathbf{K} \sqrt{u_0/2u_4}, & f(0,0) &= -u_4, \\ c &= 2a^{-3}k^{-1} \sqrt{2u_0u_4}(1-k^2)\mathbf{K}. \end{aligned} \quad (\text{III.11})$$

With σ' from Eq. (15) in [6] we have for σ as defined by (III.10)

$$\sigma = 2a^{-3}k^{-1} \sqrt{2u_0u_4} \{2\mathbf{E} - (1-k^2)\mathbf{K}\}. \quad (\text{III.12})$$

For the $(180^\circ[110]180^\circ)$ Bloch wall:

$$C = u_2(2\omega^2 + 3\omega + 2)/4\omega, \quad f(0,0) = -\frac{7}{4}u_2 \quad (\text{III.13})$$

and, from Eqs (23) and (26) in [6],

$$\Delta = 4\mathbf{K} \sqrt{u_0/2u_2(3+\omega)} \quad (\text{III.14})$$

where the function $\omega = \omega(k)$ is given by Eq. (27) in [6]. Hence

$$c = 2a^{-3} \sqrt{2u_0u_2(3+\omega)} (\omega-1)^2 \mathbf{K} / \omega(3+\omega) \quad (\text{III.15})$$

and, with σ' from Eq. (41) in [6] we obtain for σ as defined by (III.10) the formula

$$\sigma = 2a^{-3} \sqrt{2u_0u_2(3+\omega)} \left\{ 2\mathbf{E} + \frac{\omega-1}{\omega(3+\omega)} [2(\omega+1)\mathbf{II}(-\omega^{-2}, k) - (3\omega+1)\mathbf{K}] \right\}. \quad (\text{III.16})$$

For the $(90^\circ[101]180^\circ)$ Bloch wall:

$$C = u_2(10\omega^2 + 3\omega + 10)/20\omega, \quad f(0,0) = -\frac{23}{20}u_2 \quad (\text{III.17})$$

and, from Eqs (48) and (50) in [6],

$$\Delta = 4\mathbf{K} \sqrt{5u_0/2u_2(3+5\omega)} \quad (\text{III.18})$$

where the function $\omega = \omega(k)$ is given by Eq. (51) in [6]. From the above formulae we have

$$c = 10a^{-3} \sqrt{2u_0u_2(3+5\omega)/5(\omega-1)^2\mathbf{K}/\omega(3+5\omega)}. \quad (\text{III.19})$$

With σ' from Eq. (55) in [6] one has for σ as defined by (III.10)

$$\begin{aligned} \sigma = 2a^{-3} \sqrt{2u_0u_2(3+5\omega)/5} \left\{ 2\mathbf{E} + \right. \\ \left. + \frac{5(\omega-1)}{\omega(3+5\omega)} [2(\omega+1)\mathbf{II}(-\omega^{-2}, k) - (3\omega+1)\mathbf{K}] \right\}. \end{aligned} \quad (\text{III.20})$$

For the $(90^\circ[111]120^\circ)$ Bloch wall:

$$\begin{aligned} C = u_3(2-k^2)/k^2, \quad \Delta = \frac{2}{3}k\mathbf{K} \sqrt{2u_0u_3}, \quad f(0,0) = -u_3, \\ c = \frac{8}{3}a^{-3}k^{-1} \sqrt{2u_0u_3} (1-k^2)\mathbf{K}. \end{aligned} \quad (\text{III.21})$$

With σ' from Eq. (66) in [6] we obtain for σ as defined by (III.10)

$$\sigma = \frac{8}{3}a^{-3}k^{-1} \sqrt{2u_0u_3} \{2\mathbf{E} - (1-k^2)\mathbf{K}\}. \quad (\text{III.22})$$

It should be noted that for each wall the energies σ as calculated here and σ' as derived in [6] approach the same asymptotic value σ_∞ in the limit $\Delta \rightarrow \infty$, which explains why the correspondences to the asymptotic case proven in [6] (and, for that matter, in [16] too) were flawless⁴. However, while σ increases with decreasing Δ and tends to infinity for $\Delta \rightarrow 0$, Eqs (7) and (8), the opposite is true for σ' and

$$\lim_{\Delta \rightarrow 0} \sigma'(\Delta) = 0. \quad (\text{III.23})$$

This is why in the example considered in Section 6 in [6] the energy of the contracted $(90^\circ[100]90^\circ)$ Bloch wall turned out to be smaller than σ_∞ , the latter being for this particular wall equal to σ_0 as defined by Eq. (67) in [6] or by Eq. (12) in the present paper. For the same 10% contraction of the wall considered in that example, the correct formula (III.12) leads to $\sigma = 1.06 \sigma_0$ (see Table V), instead of $\sigma' = 0.8 \sigma_0$ as obtained in [6], Eq. (69).

⁴ This is not at all surprising, as in the asymptotic case $\Delta = \infty$ one imposes on the Euler-Lagrange equation the boundary conditions $\dot{\varphi} = \varphi = 0$ (or $\dot{\varphi} = 0, \varphi = \alpha$; see text following Eq. (III. 7)) at infinity which, according to Eqs (III. 4) and (III. 7), leads to $C = u_2 + u_3 + u_4 = -f(0,0)$; in which case Eqs (III. 8) and (III. 9) coincide.

REFERENCES

- [1] W. J. Ziętek, *Acta Phys. Polon.*, **25**, 117 (1964).
- [2] P. W. Neurath, C. D. Graham, *J. Appl. Phys.*, **28**, 888 (1957).
- [3] C. D. Graham, *J. Appl. Phys.*, **29**, 1451 (1958).
- [4] L. Špaček, *Ann. Phys. (Leipzig)*, **5**, 210 (1960).
- [5] M. Matlak, A. Wachniewski, *Acta Phys. Polon.*, **32**, 959 (1967).
- [6] A. Wachniewski, W. J. Ziętek, *Acta Phys. Polon.*, **32**, 21 (1967).
- [7] J. Kowalski, *Acta Phys. Polon.*, **32**, 309 (1967).
- [8] B. A. Lilley, *Phil. Mag.*, **41**, 792 (1950).
- [9] A. Wachniewski, *Acta Phys. Polon.*, **29**, 437 (1966a); **30**, 647 (1966b).
- [10] K. H. Stewart, *Ferromagnetic Domains*, Cambridge-London, University Press, 1954.
- [11] E. Kneller, *Ferromagnetismus*, Berlin-New York, Springer-Verlag, 1962.
- [12] A. Seeger (editor), *Chemische Bindung in Kristallen und Ferromagnetismus*, Berlin-New York, Springer-Verlag, 1966.
- [13] W. J. Ziętek, *Acta Phys. Polon.*, **32**, 385 (1967).
- [14] V. M. Belyakov, R. J. Kravtsova, M. T. Rappoport, *Tables of Elliptic Integrals*, Vol. I, AN SSSR, Moscow 1962 (in Russian).
- [15] M. Warmus, *Tables of Elementary Functions*, PWN, Warsaw 1960 (in Polish).
- [16] A. Wachniewski, W. J. Ziętek, *Acta Phys. Polon.*, **32**, 93 (1967).